

# TeG-DG: Textually Guided Domain Generalization for Face Anti-Spoofing

Lianrui Mu\*  
Xiaoyu Liang

Jianhong Bai\*  
Yuchen Yang

Zhejiang University

Xiaoxuan He  
Jiedong Zhuang  
Jiangnan Ye  
Haoji Hu†

mulianrui@zju.edu.cn

## Abstract

Enhancing the domain generalization performance of Face Anti-Spoofing (FAS) techniques has emerged as a research focus. Existing methods are dedicated to extracting domain-invariant features from various training domains. Despite the promising performance, the extracted features inevitably contain residual style feature bias (e.g., illumination, capture device), resulting in inferior generalization performance. In this paper, we propose an alternative and effective solution, the **Textually Guided Domain Generalization** (TeG-DG) framework, which can effectively leverage text information for cross-domain alignment. Our core insight is that text, as a more abstract and universal form of expression, can capture the commonalities and essential characteristics across various attacks, bridging the gap between different image domains. Contrary to existing vision-language models, the proposed framework is elaborately designed to enhance the domain generalization ability of the FAS task. Concretely, we first design a *Hierarchical Attention Fusion* (HAF) module to enable adaptive aggregation of visual features at different levels; Then, a *Textual-Enhanced Visual Discriminator* (TEVD) is proposed for not only better alignment between the two modalities but also to regularize the classifier with unbiased text features. TeG-DG significantly outperforms previous approaches, especially in situations with extremely limited source domain data ( $\sim 14\%$  and  $\sim 12\%$  improvements on HTER and AUC respectively), showcasing impressive few-shot performance. The code will be publicly available.

## 1. Introduction

Facial recognition technology [12, 58, 65] has become a pivotal component in various applications, including mobile device authentication [15], electronic payments [57], and cybersecurity [62]. However, the integrity of this technology is constantly under threat from various presentation decep-

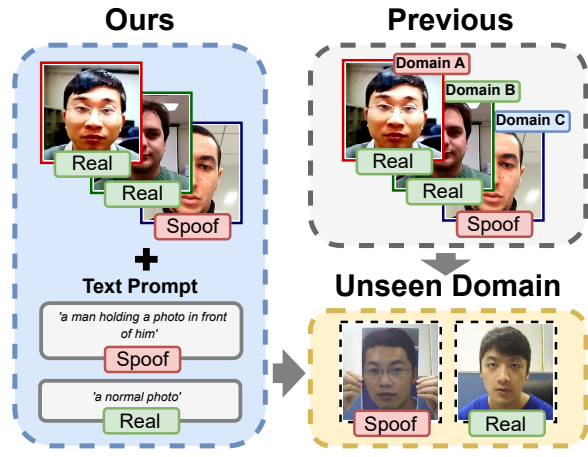


Figure 1. Comparison with previous Face Anti-Spoofing (FAS) methods. Our approach leverages the text information for better generalization *without* using domain labels.

tion, e.g. printed photo [50, 66], mask [24, 33, 43, 78], video replay [6, 8, 52, 74, 84, 85], etc. To counter these attacks, a spectrum of Face Anti-Spoofing (FAS) works [1, 47] has been proposed, leveraging either handcrafted [5, 10, 23, 41, 45, 49, 75], or deep learning features [16, 72, 76, 79–81] for spoof detecting. While these approaches demonstrate commendable test performance under intra-dataset scenarios, their generalization capability is severely compromised when confronted with unseen domains [60, 82].

To this end, recent FAS studies integrate ideas from the field of domain adaptation (DA) [25, 70, 86, 89] and domain generalization (DG) [20, 35, 36, 73, 88, 90]. Specifically, DA [39, 40, 71] aims to narrow the gap between the source and target domains by fine-tuning models with target domain samples, requiring the collection of target domain data. While DG [4, 19, 87] aims to learn universally applicable feature spaces, ensuring a consistent representation of similar categories across various domains. In general, both DA and DG encourage the model in learning *domain-invariant* features across multiple training domains. Despite their promising results, DA-based methods [21, 55, 69] still rely on a modest amount of target domain images for adaptation, which is not always available in practice [82]. On the

\*Equal contribution

†Corresponding Author

other hand, current DG-based methods [7, 60] are not supervised to learn robust features that can transfer to broader unseen domains, causing them to be deceived by the style features inherent to the limited training domains [20, 73].

In this paper, we proposed a novel and principal method to exploit the textual information to improve the generalization ability of FAS. As illustrated in Fig. 1, we supplement the single-modality visual features with text descriptions that match different types of attacks or real cases for better generalization. Our core insight is that text descriptions possess a natural universality across different domains and can be leveraged to bridge the gap between various visual domains (*e.g.*, images captured by different devices or having distinct backgrounds). However, we empirically discover that a naive migration of existing vision-language models [22, 28, 56] to FAS results in inferior performance (see Sec. 4.3 and Appendix). To this end, we devise a new framework, Textually Guided Domain Generalization (TeG-DG), to better exploit textual information for both visual feature learning and decision boundary optimization.

The pipeline of the proposed framework is illustrated in Fig. 2. TeG-DG comprises a Text Prompter (TP) to synthesize paired image-text data for training. During training, a Hierarchical Attention Fusion (HAF) module and a Textual-Enhanced Visual Discriminator (TEVD) are designed to work collaboratively to tackle the domain generalization problem in FAS. Specifically, since different attacks may affect features at different granularities, the hierarchical attention fusion module aims to adaptively merge both the local texture features and the high-level semantics of an input image. On the other hand, the textual-enhanced visual discriminator incorporates textual supervision by matching the aggregated visual features with the corresponding text descriptions, which act as prototypes of each category, and regularizing the decision boundaries of the classifier. Experimental results on various datasets demonstrate the effectiveness of TeG-DG. We also conduct comprehensive analyses to understand the designed method. In summary, the main contributions of the paper are as follows:

- *New insight.* We propose to solve the domain generalization problem in face anti-spoofing by introducing domain-invariant supervision from textual description.
- *New framework.* We design a novel yet easy-to-use FAS framework, which is composed of a hierarchical attention fusion module and a textual-enhanced visual discriminator, both of which are elaborately designed to enhance the domain generalization ability of the FAS task.
- *New scenarios and compelling empirical results.* We conducted extensive experiments on widely used benchmark datasets to verify and understand the effectiveness of the proposed method. We further extend FAS to few-shot scenarios and scenarios with extremely limited source domain data, which are more common in practice.

## 2. Related Work

**Face Anti-Spoofing** Early attempts at Face Anti-Spoofing (FAS) predominantly utilized traditional hand-crafted features such as SIFT [49], LBP [1], and HOG [41]. They primarily use color spaces and temporal information to differentiate between real and spoofed faces. The advent of deep learning, particularly Convolutional Neural Networks (CNNs), marked significant advancements in FAS. This evolution included the integration of auxiliary signals like depth maps [2, 60], r-ppg signals [45] or reflection map [77] to enhance detection capabilities. Although these techniques show promising intra-dataset performance, they exhibit severe performance degradation when applied to target datasets due to the domain shifts.

Follow-up studies improve the ability of FAS methods on domain generalization. Apart from domain adaptation-based methods [25, 70, 86, 89], meta-learning techniques [14, 35, 36, 61, 88] and domain generalization-based methods have become a promising direction in the field of FAS in recent years. Typical techniques in DG-based methods involve using adversarial learning to form compact distributions for real faces while distancing spoofed faces [20, 60, 73, 90]. In particular, MADDG [60] and SSAN [73] employed domain labels to generate assembled features to learn a domain-invariant feature space from the training domains. However, it was noted that the artificial domain labels used in these methods are coarse and do not accurately reflect the real domain distributions. Consequently, IADG [90] attempted to alleviate this issue by using an instance feature whitening method without relying on domain labels. A recent work [30] also utilizes Transformer models in FAS to achieve stronger representational capabilities. Additionally, FLIP [63] shows that direct finetuning of a multimodal pre-trained ViT to align with text prompts achieves better FAS generalizability. Compared with FLIP [63], we delve deeper into the impact of text prompts on generalization ability C.2. We use the HAF module to generate superior visual representations and do not require the involvement of text prompts during inference. Nevertheless, having access to multiple training domains is challenging in practice, which limits the application of existing methods. In this paper, we introduce a novel approach to address these issues by incorporating domain-invariant textual information into the FAS task.

**Vision-Language Models** The recent development in visual-language model (VLM) research reveals the critical role of textual data in augmenting visual task performance. Foundational VLMs like CLIP [56] and related works [17, 27–29] completed mapping images and text to a shared representation space, setting a platform in tasks for zero-shot learning and image-text classification. This confluence of modalities not only enriches the information base for these models but also addresses inherent challenges in image interpretation, such as ambiguity, noise, and the need for fine-

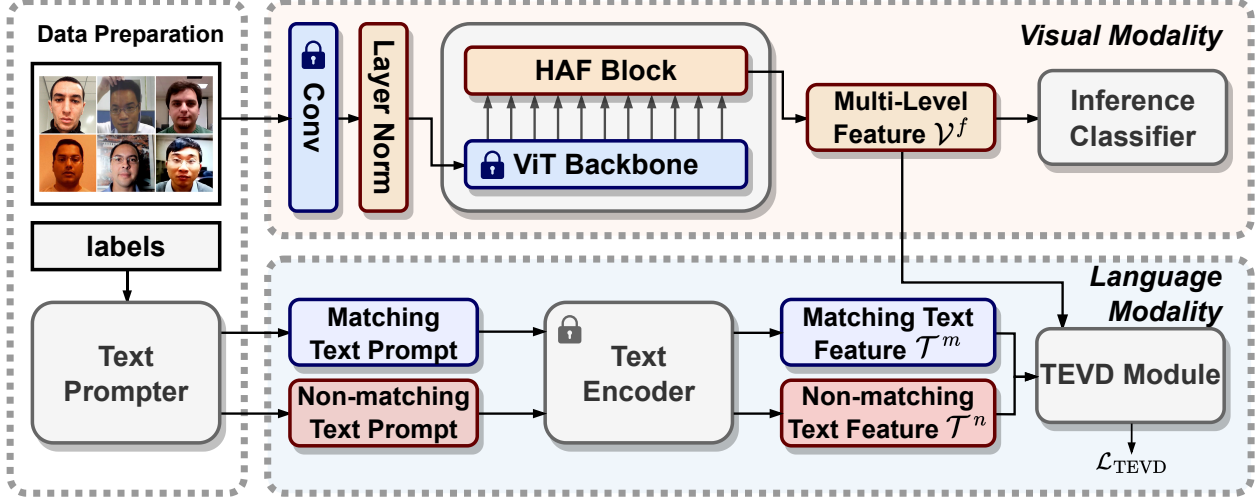


Figure 2. **Overview of the proposed Textually Guided Domain Generalization (TeG-DG) framework.** The framework contains Text Prompter (TP) for text prompt generation, the Hierarchical Attention Fusion(HAF) module for fused visual feature extraction, and the Textual-Enhanced Visual Discriminator (TEVD) for integrating text information.

grained recognition. Building upon this groundwork, a few works illustrated the potential of deeply integrated textual information in VLMs. CMA-CLIP [34] adeptly integrates sequence-wise and modality-wise attentions to synergize image and text data, thus facilitating enhanced multi-task classification. Menon *et al.* [44] leverage detailed descriptors from large language models, presenting an interpretable paradigm for image classification that significantly improves visual categorization. Lin *et al.* [32] propose a novel cross-modal adaptation method that utilizes cues from visual, textual, and audio modalities, effectively transcending the limitations of vision-only learning methods. CuPL [53] demonstrates that textual descriptions can effectively guide models in recognizing and classifying unseen objects, even in the absence of extensive training datasets. These studies underscore the capability of pre-trained visual-language models to infuse textual supervision, thereby enabling the use of textual information for improved generalization beyond the training domains. We introduce an innovative Textual-Enhanced Visual Discriminator (TEVD) module in our work, which leverages text information for classification assistance and regularization. This allows for the organic integration of features provided by the language model into the FAS task.

### 3. Textually-Guided Domain Generalization

In this section, we will present a detailed description of the proposed Textually Guided Domain Generalization (TeG-DG) framework, as illustrated in Fig. 2. In Sec. 3.1, we briefly describe the construction process of the image-text pair data for multi-modal training. In Sec. 3.2, we introduce the two main components of TeG-DG, namely, the Hierarchical Attention Fusion (HAF) module (Sec. 3.2.1) and the Textual-Enhanced Visual Discriminator (TEVD)

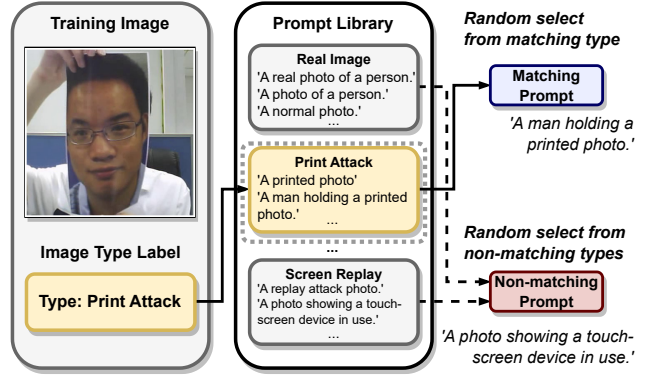


Figure 3. Text prompt generation for a training image.

(Sec. 3.2.2). They work collaboratively to learn discriminative and domain-invariant features for better generalization.

#### 3.1. Data Preparation

To incorporate domain-invariant textual information into the training process, we first design a Text Prompter (TP) module to dynamically supply matching and non-matching textual descriptions for images during training, based on the image label. As depicted in Fig. 3, for each training image, the text prompter randomly selects a matching text prompt and a non-matching text prompt from the *prompt library* for different types of images. For example, the matching text prompt to a print attack image can be *A man holding a printed photo.* while the non-matching text prompt could be *A photo of displaying a video clip on an iPad.* To ensure unbiased and diverse text prompts, we construct the *prompt library* by employing GPT-4 [46] to automatically generate semantically similar phrases, eliminating subjective bias from manually designed text prompts. For instance, in

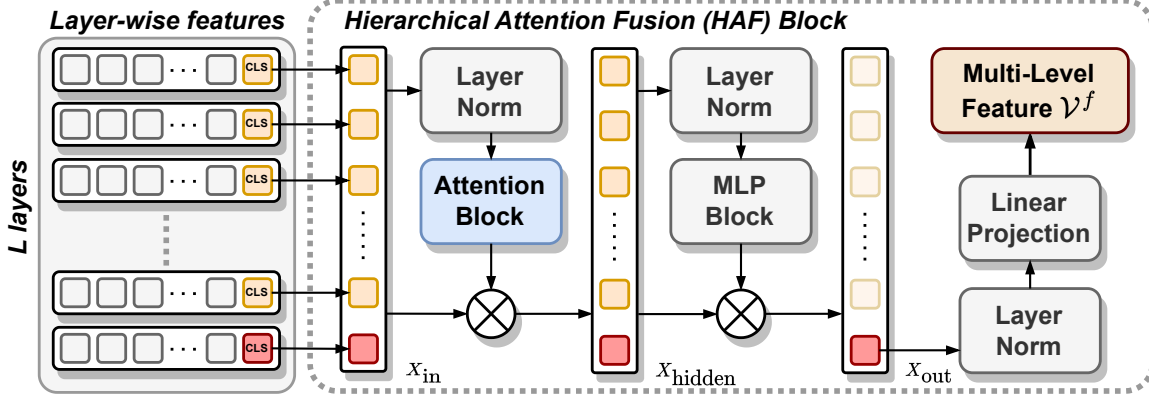


Figure 4. **Illustration of the designed Hierarchical Attention Fusion (HAF) module.** The proposed HAF is a lightweight plug-and-play module that can be easily integrated into mainstream ViT models.

the case of generating descriptive phrases for print attacks in Fig. 3, we first manually craft an initial introductory text such as A photo of a display for the replay attack. Then, we query GPT-4 with text prompts like: Write several short sentences with semantic similarity to {A photo of a display.}. The generated phrases are then added to the *prompt library* as textual descriptions of this image type (label). This approach provides diverse textual inputs to enhance the training effectiveness of the model (see Sec. 4.4).

### 3.2. Methodology

#### 3.2.1 Hierarchical Attention Fusion Module

In face anti-spoofing, different attacks may lead to feature changes at different granularities. For instance, replay attacking involves more significant changes in the low-level texture features of the image, such as the moiré patterns [48]. On the other hand, attacks like printing or masking usually alter the high-level semantics of the image. This necessitates the model to have the capability of aggregating features at different levels to cope with attacks at different scales. However, existing ViT models [13, 37, 38] typically use the [CLS] token of the last layer as the representation for recognition tasks, which makes it difficult to effectively integrate features at different levels, resulting in lower test accuracy.

To solve this problem, we propose the Hierarchical Attention Fusion (HAF) module to achieve an adaptive merge of both the local texture features and the overall semantics of an input image. Experiments in Sec. 4.4 empirically show that the designed HAF module significantly enhances ViTs in dealing with varied scales of attacks in FAS. Specifically, HAF fused information from [CLS] tokens of different layers in ViT through the self-attention block and the MLP block. Typically, for a training image  $x \in \mathbb{R}^{C \times H \times W}$ , we first divide it into  $N$  patches and feed it into a visual transformer with  $L$ -layers to obtain its layer-wise features  $Z = \{z^1, z^2, \dots, z^L\}$ , where  $z \in \mathbb{R}^{(N+1) \times D}$ . A straight-

forward solution for feature aggregation is to perform self-attention on all features in  $Z$ . Nevertheless, it is computationally expensive and will bring many learnable parameters. Hence, we turn to utilizing the [CLS] token as an alternative for feature fusion. Since the information of  $(N+1)$  token has been fused in the self-attention block of each layer, it can reduce redundancy and unnecessary operations compared to using all layer-wise features. Therefore, the input  $X_{in} \in \mathbb{R}^{L \times D}$  of the HAF module is formulated as:

$$X_{in} = (z_{[CLS]}^1, z_{[CLS]}^2, \dots, z_{[CLS]}^L)^T. \quad (1)$$

We first apply layer normalization (LN) [3] to the layer-wise feature  $X$  to alleviate internal covariate shifts caused by domain shifts. Then, the normalized features are projected with linear projections to align the dimensions of visual features with textual features, akin to the approach used in previous works [28, 31, 56] :

$$Q = \text{LN}(X_{in})W^Q \quad K = \text{LN}(X_{in})W^K \quad V = \text{LN}(X_{in})W^V \quad (2)$$

where  $W^Q, W^K, W^V \in \mathbb{R}^{D \times D}$  are learned weight matrices for projecting to  $Q$ ,  $K$ , and  $V$  spaces respectively. Then the self-attention score is calculated as:

$$\text{Attention}(Q, K, V) = \text{Softmax} \left( \frac{QK^T}{\sqrt{D}} \right) V, \quad (3)$$

where  $D$  is the dimensionality of the key (and query) in the self-attention mechanism. We also follow the common practice of implementing multi-head [68]. To enable the HAF module for capturing more complex features and patterns, we further add a multilayer perceptron (MLP) and residual connections [18] subsequently:

$$\begin{cases} X_{hidden} = \text{Attention}(Q, K, V) + X_{in} \\ X_{out} = \text{MLP}(\text{LN}(X_{hidden})) + X_{hidden} \end{cases} \quad (4)$$

Finally, we extract the normalized fused vision features from the last layer and map its dimension to the text feature with a learnable projection matrix  $M \in \mathbb{R}^{D_{out} \times D}$  for cross-modal alignment (will be introduced in Sec. 3.2.2):

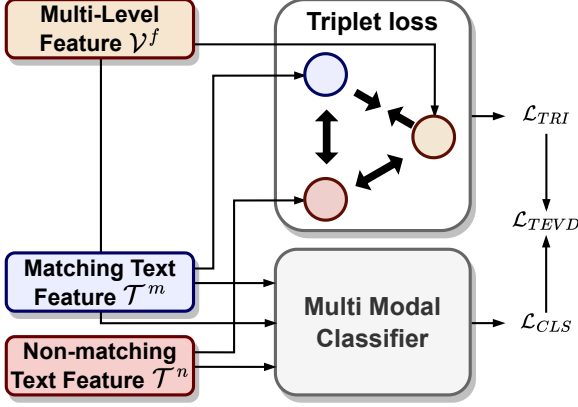


Figure 5. **The proposed textual-enhanced visual discriminator (TEVD).** TEVD consists of a vision-language triplet loss and a multi-modal classifier.

$$\mathcal{V}^f = \text{LN}(X_{\text{out}}^{(L)}) \cdot M. \quad (5)$$

The obtained visual feature  $\mathcal{V}^f$  is aggregated with multi-level features from each layer of the ViT model, thereby capable of detecting various attacks at different granularities.

### 3.2.2 Textual-Enhanced Visual Discriminator

To effectively integrate the text information into the training process, we further design a Textual-Enhanced Visual Discriminator (TEVD), which includes a vision-language triplet loss and a multi-modal classifier. We also make a detailed discussion and comparison between the proposed TEVD and the widely-used CLIP [56] strategy in Tab. 3.

**Vision-Language Triplet loss.** We return to our core insight – text can naturally capture the commonalities and essential characteristics across various attacks, thus bridging the gap between different image domains. To learn domain-invariant visual features, we leverage text features as supervision, guiding the model to filter out the inherent noise and domain-specific features (e.g., illumination, background) in visual representations. Concretely, a vision-language triplet loss is designed to achieve cross-modal alignment, where the text features can be interpreted as the prototypes of visual representations. It also results in more compact real-face features and distances the features of attack images from those of real ones, thereby improving the model’s generalization ability to unknown domains. We also conduct studies when implementing the contrastive loss in the Appendix.

To apply vision-language triplet loss, we first extract the visual multi-level feature  $\mathcal{V}^f$  from input image  $x$  through our HAF module (introduced in Sec. 3.2.1), along with extracting the image’s matching and non-matching text prompt feature  $\mathcal{T}^m$  and  $\mathcal{T}^n$  through text encoder. After L2 normalization, we form these features as a triplet  $(\mathcal{V}_{\text{Norm}}^f, \mathcal{T}_{\text{Norm}}^m, \mathcal{T}_{\text{Norm}}^n)$  for optimizing. The goal of the triplet loss  $\mathcal{L}_{\text{TRI}}$  is to ensure

---

#### Algorithm 1 The Hierarchical Attention Module.

---

```

1: Input: Concatenate [CLS] tokens  $X_{\text{in}}$ .
2: Output: Extracted fused vision feature.  $\mathcal{V}^f$ 
3: function HAF_MODULE( $X_{\text{in}}$ )
4:   # Calculate features through attention and mlp
5:    $X_{\text{hidden}} = \text{Attention}(\text{LN}(X_{\text{in}})) + X_{\text{in}}$ 
6:    $X_{\text{out}} = \text{MLP}(\text{LN}(X_{\text{out}})) + X_{\text{out}}$ 
7:   # Project the vector dimensions to  $D_{\text{out}}$ 
8:    $\mathcal{V}^f = \text{LN}(X_{\text{out}}^{(L)}) \cdot M$ 
9:   return  $\mathcal{V}^f$ 
10: end function

```

---

#### Algorithm 2 The Textual-Enhanced Visual Discriminator.

---

```

1: Input: training images  $x$ , image binary label  $y$ , image types  $types$ .
2: Output: TEVD module calculated loss  $\mathcal{L}_{\text{TEVD}}$ .
3: function TEVD_MODULE( $x, y, types$ )
4:   # Generate matching and non-matching text prompts
5:    $P_m, P_n = \text{TextPrompter}(types)$ 
6:   # Extract image and text features
7:    $\mathcal{V}^f = \text{VisionEncoder}(x)$ 
8:    $\mathcal{T}^m = \text{TextEncoder}(P_m)$ 
9:    $\mathcal{T}^n = \text{TextEncoder}(P_n)$ 
10:  # L2 normalize then concatenate
11:   $\mathcal{V}_{\text{Norm}}^f, \mathcal{T}_{\text{Norm}}^m, \mathcal{T}_{\text{Norm}}^n = \text{Normalize}(\mathcal{V}^f, \mathcal{T}^m, \mathcal{T}^n)$ 
12:   $features = \text{Cat}(\mathcal{V}_{\text{Norm}}^f, \mathcal{T}_{\text{Norm}}^m, \mathcal{T}_{\text{Norm}}^n)$ 
13:   $labels = \text{Cat}((y, y, \text{Invert}(y)))$ 
14:  # Classification through multi-modal classifier  $g$ 
15:   $scores = g(features)[:, 1]$ 
16:  # Cross entropy loss and triplet loss
17:   $\mathcal{L}_{\text{CLS}} = \text{CrossEntropyLoss}(scores, labels)$ 
18:   $\mathcal{L}_{\text{TRI}} = \text{TripletsLoss}(\mathcal{V}_{\text{Norm}}^f, \mathcal{T}_{\text{Norm}}^m, \mathcal{T}_{\text{Norm}}^n)$ 
19:   $\mathcal{L}_{\text{TEVD}} = \mathcal{L}_{\text{CLS}} + \lambda \mathcal{L}_{\text{TRI}}$ 
20:  return  $\mathcal{L}_{\text{TEVD}}$ 
21: end function

```

---

that  $\mathcal{V}_{\text{Norm}}^f$  is closer to  $\mathcal{T}_{\text{Norm}}^m$  than  $\mathcal{T}_{\text{Norm}}^n$ :

$$\mathcal{L}_{\text{TRI}} = \max(0, D(\mathcal{V}_{\text{Norm}}^f, \mathcal{T}_{\text{Norm}}^m) - D(\mathcal{V}_{\text{Norm}}^f, \mathcal{T}_{\text{Norm}}^n) + \alpha), \quad (6)$$

where  $D(\mathcal{V}_{\text{Norm}}^f, \mathcal{T}_{\text{Norm}}^m)$  denotes the Euclidean distance between  $\mathcal{V}_{\text{Norm}}^f$  and  $\mathcal{T}_{\text{Norm}}^m$ , and  $\alpha$  is a predefined margin.

**Multi-Modal Classifier.** To enhance the domain generalization ability in FAS, we hope to learn a classifier that can make reasonable judgments based on the consistent features across domains, and automatically discard the noise or the domain-specific details that may exist in the visual representations. To this end, we design a multi-modal classifier by classifying visual representations as well as corresponding matching and non-matching text prompt features simultaneously. The multi-modal classifier enriches the representation of the visual feature space and aligns visual features with the

textual representation feature space. In other words, since the low-level textures and noise information are not involved in the pre-trained text feature, it serves as the regularization term to prevent overfitting of the classifier. Note that the language modality is removed during inference.

To better align the textual and visual features, we ensure that the prompt features corresponding to the input image labels are classified into the same category, while the non-matching prompt features are classified into the opposite category. Consider the binary label  $y$  of the input image  $x$ , we use  $\neg y$  to represent the opposite label of  $y$ , and the multi-modal classifier is represented as  $g$ . The optimization objective is as follows:

$$\begin{aligned}\mathcal{L}_{\text{CLS}} = & -(y \log(g(\mathcal{V}_{\text{Norm}}^f)) + \neg y \log(1 - g(\mathcal{V}_{\text{Norm}}^f))) \\ & -(y \log(g(\mathcal{T}_{\text{Norm}}^m)) + \neg y \log(1 - g(\mathcal{T}_{\text{Norm}}^m))) \\ & -(y \log(1 - g(\mathcal{T}_{\text{Norm}}^n)) + \neg y \log(g(\mathcal{T}_{\text{Norm}}^n)))\end{aligned}\quad (7)$$

In summary, TeG-DG first applies the hierarchical attention fusion module to obtain enhanced multi-level visual representations, and further regularize the learned decision boundaries by the designed textual-enhanced visual discriminator. The overall loss function of TeG-DG during training is as follows:

$$\mathcal{L}_{\text{TeG-DG}} = \mathcal{L}_{\text{CLS}} + \lambda \mathcal{L}_{\text{TRI}}, \quad (8)$$

where  $\lambda$  is a hyper-parameter. The PyTorch-style pseudo-code of HAF and TEVD is summarized in Alg. 1 and Alg. 2. The algorithm of TeG-DG is presented in the Appendix.

## 4. Experiment

### 4.1. Experimental Settings

**Datasets.** We evaluate the proposed method across four publicly available datasets [6, 8, 74, 85], each manifesting significant domain variations (*e.g.*, illumination, resolution, capture device, *etc.*), especially for the spoof ones, which is highly suitable for DG-FAS experiments. These datasets are OULU-NPU [6] (denoted as O), Replay-Attack [8] (denoted as I), MSU-MFSD [74] (denoted as M), and CASIA-MFSD [85] (denoted as C). To ensure a *fair* comparison, we follow the same protocols employed by previous DG-based FAS methods [20, 35, 36, 60, 61, 88, 90] in all our experiments.

**Evaluation Metrics.** We use the Half Total Error Rate (HTER) [9] and the Area Under Curve (AUC) for evaluation. HTER is a metric to evaluate the performance of a face anti-spoofing model, which is the average of the false acceptance rate (FAR) and the false rejection rate (FRR), measures the proportion of spoofing attacks and genuine faces that are incorrectly classified by the system. AUC aims to evaluate the performance of a binary classifier. It measures the area under the Receiver Operating Characteristic (ROC) curve,

which plots the true positive rate against the false positive rate at different threshold values.

### 4.2. Comparisons to State-of-the-Art

**Leave-One-Out.** In alignment with previous researches [14, 20, 35, 36, 60, 73, 88, 90], we adopted the same Leave-One-Out (LOO) protocol for our experiments. Detailed comparative results are thoroughly documented in Tab. 1. Under the LOO protocol, three datasets are chosen to serve as source domains, while the remaining dataset is designated as the unseen target domain, not accessible during training. We compare different FAS methods in Tab. 1 including traditional FAS approaches [11, 42] that exhibit subpar performance in domain generalization, as well as domain generalization FAS methods [7, 14, 20, 26, 30, 35, 60, 61, 73, 88, 90] that do not incorporate textual supervision. Our methodology, integrating textual supervision, outshines nearly all existing domain generalization frameworks under the LOO protocol. By aligning features with abstract textual space, our model, despite its simpler architecture, excels over more intricate systems that depend on feature whitening transformations and domain alignment and demonstrates significant improvements over these traditional methods.

**Limited source domains.** We also evaluate our method in scenarios with extremely limited source domains. Following previous works [20, 35, 60, 90], MSU-MFSD (M) and ReplayAttack (I) are selected as the source domains for training, while the remaining CASIA-MFSD (C) and OULU-NPU (O) datasets will be used as the target domains for testing respectively. The result is shown in Tab. 2. Our TeG-DG method significantly outperforms state-of-the-art approaches, showing  $\sim 14\%$  and  $\sim 12\%$  improvements on HTER and AUC respectively. Notably, it outperforms most traditional domain generalization (DG) models, even those trained on a wider range of source datasets when testing on CASIA-MFSD. And even outperform all the methods we listed in Tab. 1 when testing on OULU-NPU. Our approach does not require domain labels and leverages the inherent abstract information provided by text, yielding better performance with fewer training domains. Given the practical challenges of acquiring sufficient source domain FAS data in real-world settings, the superior performance of our method with fewer source domains indicates the substantial value of text supervision for generalization in FAS tasks.

### 4.3. Few-Shot Performance

Gathering diverse attack samples for Facial Anti-Spoofing (FAS) tasks is strenuous and complex. Thus, it is extremely advantageous if we have a model with robust few-shot learning capabilities. In contrast to previous few-shot methods which rely on training models on known datasets and then performing few-shot learning on unseen domains [51, 54], we have adopted a more stringent Leave-One-Out (LOO)

Table 1. **Test HTER (↓) and AUC (↑) of FAS methods on OIMC datasets.** The \* indicates using the CelebA-Spoof [83] as the supplementary source dataset (**bold** indicates best performance, underline indicates second best performance.)

Methods	I&C&M to O		O&C&M to I		O&C&I to M		O&M&I to C	
	HTER(%)	AUC(%)	HTER(%)	AUC(%)	HTER(%)	AUC(%)	HTER(%)	AUC(%)
LBPTOP [11]	53.15	44.09	49.45	49.54	36.90	70.80	42.60	61.05
MS_LBP [42]	50.29	49.31	50.30	51.64	29.76	78.50	54.28	44.98
MMD-AAE [26]	40.98	63.08	31.58	75.18	27.08	83.19	44.59	58.29
MADDG [60]	27.98	80.02	22.19	84.99	17.69	88.06	24.50	84.51
RFM [61]	16.45	91.16	17.30	90.48	13.89	93.98	20.27	88.16
SSDG-M [20]	25.17	81.83	18.21	94.61	16.67	90.47	23.11	85.45
D <sup>2</sup> AM [7]	15.27	90.87	15.43	91.22	12.70	95.66	20.98	85.58
DRDG [36]	15.63	91.75	15.56	91.79	12.43	95.81	19.05	88.79
ANRL [35]	15.67	91.90	16.03	91.04	10.83	96.75	17.85	89.26
SSAN-M [73]	19.51	88.17	14.00	94.58	10.42	94.76	16.47	90.81
AMEL [88]	11.31	93.96	18.60	88.79	10.23	96.62	11.88	94.39
DBDG [14]	15.66	92.02	18.69	92.28	9.56	97.17	18.34	90.01
SA-FAS [64]	10.00	96.23	6.58	97.54	5.95	96.55	8.78	95.37
IADG [90]	<u>8.86</u>	<u>97.14</u>	10.62	94.50	5.41	98.19	8.70	96.44
DiVT-M [30]	13.06	94.04	<u>3.71</u>	<u>99.29</u>	<u>2.86</u>	<u>99.14</u>	<u>8.67</u>	<u>96.92</u>
TeG-DG (ours)	<b>5.68</b>	<b>97.92</b>	<b>3.21</b>	<b>99.63</b>	<b>1.88</b>	<b>99.72</b>	<b>3.17</b>	<b>99.79</b>
FLIP-MCL* [63]	<b>2.31</b>	<u>99.63</u>	<u>4.25</u>	<u>99.07</u>	<u>4.95</u>	<u>98.11</u>	<u>0.54</u>	<u>99.98</u>
TeG-DG* (ours)	2.53	<b>99.76</b>	<b>2.38</b>	<b>99.69</b>	<b>1.06</b>	<b>99.99</b>	<b>0.40</b>	<b>99.99</b>

Table 2. Results on extremely limited source domains.

Methods	M&I to C		M&I to O	
	HTER(%)	AUC(%)	HTER(%)	AUC(%)
LBPTOP [11]	45.27	54.88	47.26	50.21
MS_LBP [42]	51.16	52.09	43.63	58.07
MADDG [60]	41.02	64.33	39.35	65.10
SSDG-M [20]	31.89	71.29	36.01	66.88
D <sup>2</sup> AM [7]	32.65	72.04	27.70	75.36
DRDG [36]	31.28	71.50	33.35	69.14
ANRL [35]	31.06	72.12	30.73	74.10
SSAN-M [73]	30.00	76.20	29.44	76.62
EBDG [14]	27.97	75.84	25.94	78.28
AMEL [88]	24.52	82.12	19.68	87.01
IADG [90]	24.07	85.13	<u>18.47</u>	<u>90.49</u>
DiVT-M [30]	20.11	86.71	23.61	85.73
TeG-DG (ours)	<b>6.19</b>	<b>98.64</b>	<b>6.89</b>	<b>97.49</b>

few-shot protocol, similar to the one detailed in Section 4.2. However, we differ in that we utilize only a limited number of images for training and employ a zero-shot approach for the unseen domain. To demonstrate the effectiveness of our approach in zero/few-shot learning, we conducted a comparison with ‘ViT-L/14’ CLIP [56]. The results are shown in Tab. 3, where ‘ $n$  sample’ denotes  $n$  spoofing and  $n$  real samples from each source domain, and ‘zero-shot’ indicates no image samples given. For the zero-shot scenario, our method only activates the multi-modal classifier, and CLIP classifies only via text prompts. For few-shot learning, we use a linear probe to finetune the classification head of CLIP. As train-

ing samples increase, both our method and CLIP show an expected overall improvement in classification ability. However, our approach consistently outperforms CLIP. It is also noteworthy that our model, using only a few samples from the source domain, achieved performance surpassing most DG FAS methods in Tab. 1 which completely use the whole source domain. Our superior results demonstrate the value of utilizing textual information for generalization.

#### 4.4. Analysis and Ablation Study

**The effectiveness of proposed components.** We conducted an ablation study to evaluate the performance contribution of each component in our framework, *i.e.*, the HAF module (denoted as HAF), the triplet loss in the TEVD module (denoted as triplet), and the textual guidance in TEVD module (denoted as text). The results are shown in Tab. 4. It’s observed that a total loss of textual information will harm the performance more than the absence of the triplet loss in TEVD. The HAF module effectively enhances the model’s performance on datasets with lower image quality, demonstrating its improved capability in feature extraction across images of varying quality. Each component of TeG-DG contributes to improving the performance across various architectures. Finally, the combination of all the proposed components yields the best results.

**Grad-CAM Visualization.** To provide a better understanding of TeG-DG, we further identify the regions that influence the classification results. We used Grad-CAM [59] for activation map visualization on input images. The left

Table 3. Zero-shot and few-shot performance evaluated on Leave-One-Out (LOO) protocol.

Methods	I&C&M to O		O&C&M to I		O&C&I to M		O&M&I to C	
	HTER(%)	AUC(%)	HTER(%)	AUC(%)	HTER(%)	AUC( $\uparrow$ )	HTER(%)	AUC(%)
CLIP (zero-shot)	60.35	37.23	58.73	39.09	51.84	42.12	51.02	50.12
TeG-DG (zero-shot)	<b>41.05</b>	<b>61.67</b>	<b>34.44</b>	<b>68.57</b>	<b>22.69</b>	<b>78.17</b>	<b>38.64</b>	<b>61.93</b>
CLIP (1 sample)	16.48	90.64	18.21	88.41	<b>22.24</b>	<b>88.73</b>	32.45	76.02
TeG-DG (1 sample)	<b>6.34</b>	<b>98.45</b>	<b>13.16</b>	<b>95.22</b>	27.88	85.56	<b>7.70</b>	<b>98.26</b>
CLIP (5 sample)	11.74	94.43	16.99	90.11	10.22	96.86	19.85	89.75
TeG-DG (5 sample)	<b>11.32</b>	<b>95.38</b>	<b>9.69</b>	<b>97.01</b>	<b>5.56</b>	<b>99.01</b>	<b>4.16</b>	<b>99.59</b>

Table 4. Evaluations of different components of the proposed TeG-DG framework.

Methods	I&C&M to O		O&C&M to I		O&C&I to M		O&M&I to C	
	HTER(%)	AUC(%)	HTER(%)	AUC(%)	HTER(%)	AUC( $\uparrow$ )	HTER(%)	AUC(%)
TeG-DG w/o HAF	9.86	95.87	13.16	94.35	3.23	99.51	14.34	92.26
TeG-DG w/o triplet	11.65	94.75	9.44	97.40	5.11	99.02	8.68	97.40
TeG-DG w/o text	10.71	94.90	16.13	89.99	6.99	97.50	7.09	97.92
TeG-DG (ours)	<b>5.68</b>	<b>97.92</b>	<b>7.65</b>	<b>98.67</b>	<b>1.88</b>	<b>99.72</b>	<b>3.17</b>	<b>99.79</b>

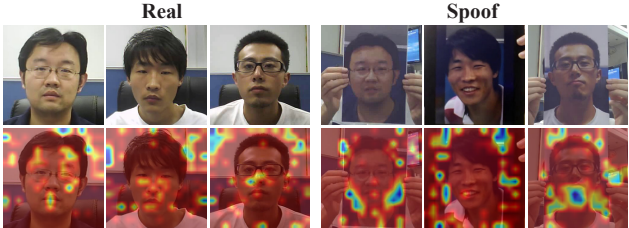


Figure 6. The Grad-CAM [59] visualizations of our TeG-DG method under protocol O&M&I to C.

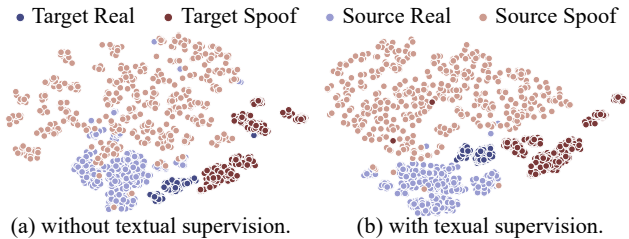


Figure 7. The t-SNE feature visualization on O&M&I to C. We plot the visual feature distribution w/ and w/o TeG-DG.

side of Fig. 6 shows the real images, while the right side shows the spoof ones. The first line and second lines refer to the input images and the corresponding activation maps, respectively. The proposed method primarily emphasizes the internal regions of real faces as cues for classification, while for attack images, the focus is more scattered to attack indicators such as photo edges and screen-caused features. This demonstrates the strong capability of TeG-DG to distinguish real and counterfeit features in unseen domains.

**t-SNE Visualization.** Figure 7 displays the t-SNE fea-

ture visualization for protocol O&M&I to C [67] with and without TeG-DG, showcasing the impact of textual supervision information. These textual supervisions facilitate a more pronounced separation in the feature space between real and spoof faces, simultaneously achieving denser and more generalized clustering of real face features. In the absence of textual supervision, the distinction between real and spoof features within the source and target domain becomes blurred. This contrast is especially noticeable when comparing the separation extent in target domain features with and without textual supervision. The t-SNE visualization of the TeG-DG feature distribution demonstrates the enhanced generalization capability of our framework, highlighting the clear advantages of integrating textual supervision.

## 5. Conclusion and Limitations

In this paper, we introduced the Textually Guided Domain Generalization (TeG-DG) framework which utilizes the natural cross-domain universality of text and leverages it to bridge the gap between various visual domains, thereby enhancing domain generalization performance. We develop the Hierarchical Attention Fusion (HAF) module to merge both the local and the high-level semantics in the visual modality and a Textual-Enhanced Visual Discriminator (TEVD) incorporates textual supervision in the language modality. Comprehensive experiments on benchmark datasets demonstrate the superiority of our approach. There are nevertheless some limitations. First, our method requires labeling spoofing attack types, which may sometimes necessitate special annotations. Second, the creation of the *prompt library* would impact the performance. We hope our work can promote the research on domain generalization FAS tasks.

## A. Data Preparation

### A.1. Dataset Construction

In alignment with standard practices in Face Anti-Spoofing (FAS) research, we adopted the same Leave-One-Out (LOO) protocol for our experiments. Under the LOO protocol, three datasets are chosen to serve as source domains, while the remaining dataset is designated as the unseen target domain, not accessible during training. We also evaluate our method in scenarios with extremely limited source domains. The dataset for LOO test and extremely limited source domains test is listed in Tab. 5. During the training phase, we maintain a balanced approach by sampling an equal number of real and spoof samples. This balance is crucial for training our system to accurately distinguish between real and spoof images under varied conditions. The datasets employed in our study are:

**OLULU-NPU:** This dataset mimics real-world variations in mobile face presentation attacks, encompassing diverse environmental conditions, lighting variations, and a range of mobile devices.

**Replay-Attack:** This dataset offers an extensive collection of video replay attacks, making it invaluable for testing the effectiveness of low level features in identifying such spoofing attempts.

**MSU-MFSD:** This dataset focused on face spoof detection using image distortion analysis, it includes a variety of spoof attacks, highlighting the importance of image quality and distortion in detecting fraud.

**CASIA-MFSD:** This dataset is renowned for its diverse spoofing attacks, it includes methods like warped photo attacks, cut photo attacks, and video replays, providing a comprehensive assessment platform for anti-spoofing systems.

Table 5. Four datasets for Leave-One-Out test.

Dataset	Live/Spoof	Attack Types
CASIA-MFSD [85]	150/450	Print, Replay
REPLAY-ATTACK [8]	200/1000	Print, Replay
MSU-MFSD [74]	70/210	Print, Replay
OLULU-NPU [6]	720/2880	Print, Replay

### A.2. Prompts Preparation

We construct the *prompt library* by employing GPT-4 [46] to generate semantically similar phrases automatically. We first manually craft an initial introductory text such as A photo of a display for the replay attack. Then, we query GPT-4 with text prompts like: Write several short sentences with semantic similarity to {A photo of a display.}. We query GPT-4 with the following text for batch generation: Write {64} numbered sentences with semantic similarity to {A photo of

---

### Algorithm 3 The train process of TeG-DG.

**Input:** Train set  $\mathcal{D}$ , hyper-parameter  $\lambda$ , train epoch  $T$ , pre-defined prompt library  $PL$ .

**Output:** Trained model parameter  $\theta_T$ .

**Initialize:** Load “ViT-L/14” CLIP [56] pre-trained parameters for the backbone in as the backbone for both the vision and language modalities of our model. The classifier in the TEVD module and parameters in the HAF module are randomly initialized.

- 1: Build up LOO dataset from  $\mathcal{D}$
- 2: Load pre-trained parameters to model
- 3: Freeze backbone model parameters except for `ln_pre` and `ln_post` in ViT
- 4: **for** epoch = 0, …,  $T - 1$  **do**
- 5:     Get training images  $x$ , binary label  $y$  and image types  $types$  from  $\mathcal{D}$ , and do pre-processing
- 6:     Train model parameter  $\theta_T$  though  $\mathcal{L}_{TEVD}$  (Sec. 3.2.2)
- 7: **end for**
- 8: Save model parameter  $\theta_T$

---

### Algorithm 4 The test process of TeG-DG.

**Input:** Unseen domain test set  $\mathcal{D}^t$ , trained model parameter  $\theta_T$

**Output:** HTER and AUC (Sec. 4).

- 1: `ScoreList` = []
- 2: `LabelList` = []
- 3: **for**  $x_i, y_i \in \mathcal{D}^t$  **do**
- 4:     Obtain the classification score  $s_i$  of  $x_i$  via the visual part of the model (Sec. 3.2.1).
- 5:     Add  $s_i$  to `ScoreList`
- 6:     Add  $y_i$  to `LabelList`
- 7: **end for**
- 8: Evaluate model with HTER and AUC through `ScoreList` and `LabelList`

---

a display.}. In this way, we generate 64 text prompts for each type of image included in adopted datasets. The generated text prompts are then added to the *prompt library* as textual descriptions of this image type. The text prompts used in the *prompt library* are listed in Page 14. During training, these will be dynamically selected as matching or non-matching text prompts to pair with training images.

### B. Pseudo-code of TeG-DG Framework

Our TeG-DG framework is designed to simultaneously engage both visual and language modalities during the training phase to max out domain generalization ability, offering a multi-faceted approach to learning. Key to this process is the Hierarchical Attention Fusion (HAF) module, which adeptly merges local texture features with high-level semantics extracted from input images. The HAF module is detailed in

Sec. 3.2.1, with its pseudo-code presented in Alg. 1.

In tandem with HAF, our framework features the Textual-Enhanced Visual Discriminator (TEVD), a crucial component in tackling the challenges of domain generalization through textual supervision. The TEVD's role and functionalities are extensively discussed in Sec. 3.2.2, and its pseudo-code is presented in Alg. 2. The training phase of the visual modality in our framework not only utilizes real/spoof image labels but also incorporates textual information to enrich the learning process.

This multi-modal training approach is encapsulated in Alg. 3, which details the pseudo-code for the entire training procedure. And during the inference stage, our framework pivots to focus exclusively on the visual modality. The language modality, pivotal during training, is set aside in this phase. For inference purposes, we utilize a multi-modal classifier, which has been trained with text regularization in the TEVD module. This inference process is detailed in Alg. 4, outlining the complete pseudo-code of inference process.

## C. More Experiment and Analysis

### C.1. Comparison to Baseline Method

Our TeG-DG framework utilizes a pre-trained Visual Language Model (VLM), but the VLM model that was not specifically designed for FAS tasks performs poorly. For example, the CLIP model exhibits a lack of specific knowledge pertinent to Face Anti-Spoofing (FAS) tasks. In the context of the four given datasets, it tends to mistakenly classify images with sharp visuals as authentic and those with blurred details as attacks, thereby overlooking other critical FAS features such as moiré patterns and loss of facial details as shown in Fig. 8. This oversight leads to misjudgments. Consequently, CLIP in its standalone form underperforms in FAS tasks.

To validate the effectiveness of our approach compared to the direct application of Vision-Language Models (VLMs), we used CLIP[56] as a baseline for comparison. We added BLIP[28] for more comprehensive measurement. Our experiments demonstrate that our method holds advantages over several alternative strategies, including using a VLM model directly, fine-tuning a VLM with a classification head, or employing contrastive loss fine-tuning with a VLM. These results are listed in Tab. 6 and underscore the superiority of our methodology in leveraging vision-language synergies.

### C.2. Impact of Different Numbers of Prompts

Our framework employs a prompt library to store currently used, predefined text prompts, and the number of these prompts can significantly impact the achievable results. To explore the effects of using different numbers of prompts, we extracted  $n$  text prompts for each image category to perform Leave-One-Out (LOO) tests, investigating the variations in Half Total Error Rate (HTER) and Area Under the Curve

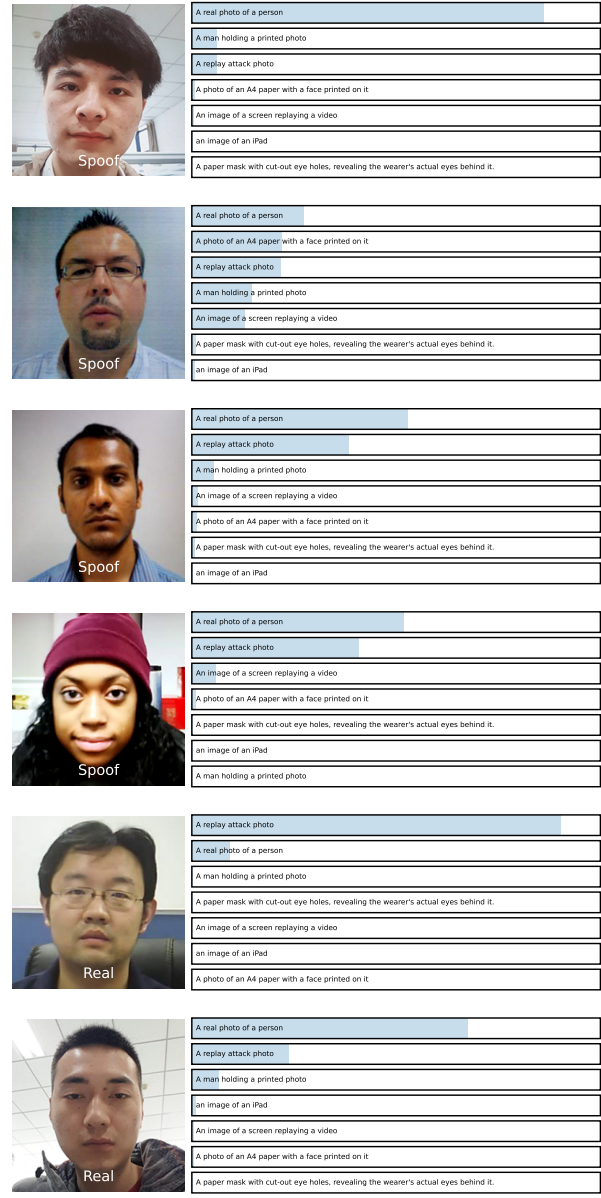


Figure 8. CLIP model lacks the knowledge of FAS tasks.

(AUC) to determine the influence of varying prompt quantities. The experimental results are shown in Fig. 14, Fig. 15, Fig. 16 and Fig. 17. It reveals that in most cases, employing a larger number of prompts tends to lower the HTER and increase the AUC. This improvement is attributed to the richer textual feature space, which overall enhances the model's generalization performance. The appropriate quantity of text prompts is beneficial within our framework, and selecting an optimal number of text prompts is essential for maximizing the performance within our framework. Based on these findings, we chose to use 64 text prompts in our previous experiments. This decision was made to leverage the

Table 6. **Comparison to Baseline Method.** ‘(Linear)’ means only using a linear classification head.

Methods	I&C&M to O		O&C&M to I		O&C&I to M		O&M&I to C	
	HTER(%)	AUC(%)	HTER(%)	AUC(%)	HTER(%)	AUC(↑)	HTER(%)	AUC(%)
CLIP (zero-shot)	60.35	37.23	58.73	39.09	51.84	42.12	51.02	50.12
CLIP (Linear)	11.03	94.80	12.50	93.97	2.78	99.69	8.68	97.18
BLIP (Linear)	23.21	80.82	16.93	87.23	12.87	94.26	27.45	78.71
contrastive Loss	6.54	98.07	8.29	98.66	3.84	99.65	7.24	98.20
TeG-DG (ours)	<b>5.68</b>	<b>97.92</b>	<b>3.21</b>	<b>99.63</b>	<b>1.88</b>	<b>99.72</b>	<b>3.17</b>	<b>99.79</b>

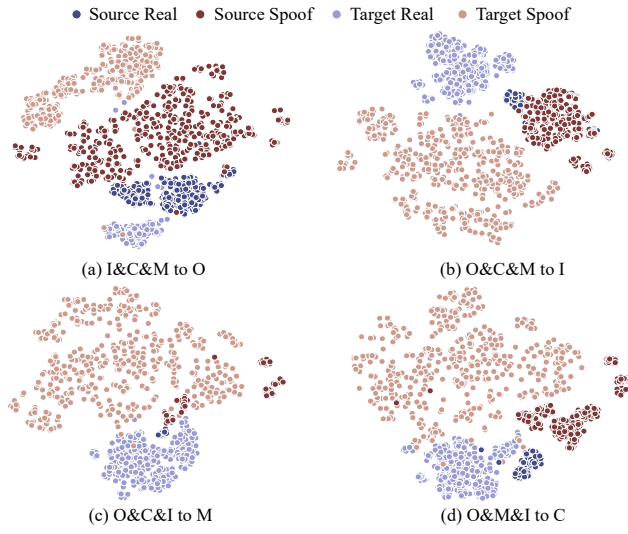


Figure 9. The t-SNE feature visualization on four LOO tests.

benefits of a richer textual feature space while maintaining operability and effectiveness in our model’s performance.

## D. Visualization

We provide more Grad-Cam [59] visualization TeG-DG in Fig. 10, Fig. 11, Fig. 12, Fig. 13. The visualization shows that our framework places a primary emphasis on the internal regions of real faces, utilizing these areas as key indicators for classification. In contrast, when analyzing spoof images, the attention is more dispersed, concentrating on tell-tale signs of spoofing such as the edges of photos and features induced by screens. The results show the strong capability of TeG-DG to distinguish real and spoof features in unseen domains on the four datasets.

We further elucidate the efficacy of the Textually Guided Domain Generalization (TeG-DG) framework through detailed t-SNE visualizations [67] across four LOO tests in Fig. 9. These visualizations are instrumental in illustrating the practical impact of textual supervision on feature distribution and domain generalization. They facilitate a more pronounced separation in the feature space between real and

spoof faces, while simultaneously achieving denser and more generalized clustering of real face features.

## E. Future Works

In our future work, we aim to advance the field of Face Anti-Spoofing (FAS) through several innovative approaches. A key area of focus will be the development of methods for automatically generating appropriate text prompts for each training sample, rather than selecting them from the prompt library according to the type label of the image. This individualized approach to prompt generation is expected to enhance the effectiveness of our current framework.

Another critical aspect of our research will involve an in-depth investigation into the impact of various text prompts on training outcomes. We intend to identify the characteristics that make a text prompt effective or ineffective. Understanding the nuances of how different prompts influence training is essential for grasping the mechanics of prompt effectiveness in our system. Additionally, we plan to address the challenges of instability that arise from diverse combinations of text prompts.

Another pivotal aspect of our future work will involve integrating traditional domain generalization FAS techniques [20, 30, 60, 73, 90] with text-supervised methods. This integration is anticipated to further enhance the performance of our models, leveraging the strengths of both domain generalization and text-based approaches to create more robust and efficient FAS systems.

Overall, our future endeavors aim to push the boundaries of domain generalization in face anti-spoofing, using text as a powerful tool to achieve superior model performance and understanding ability.

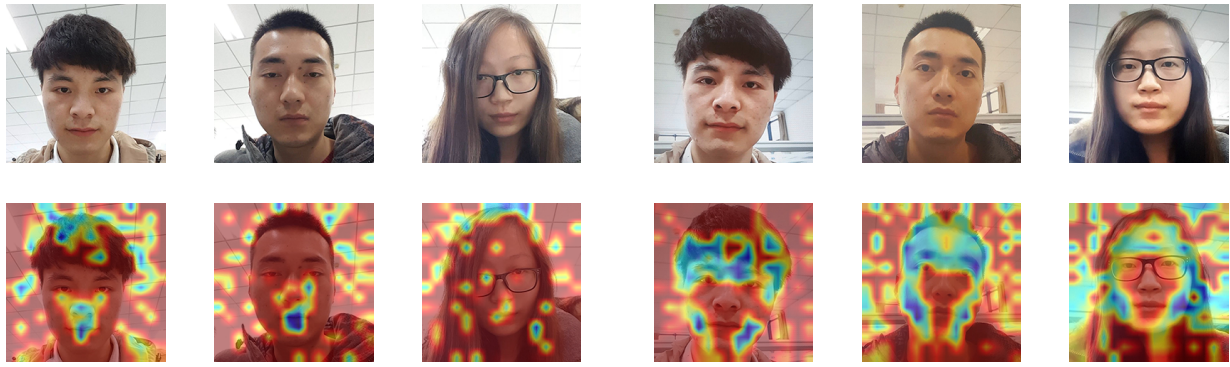


Figure 10. **Grad-Cam visualization for I&C&M to O.** On the left is a real image, and on the right is a spoof image.

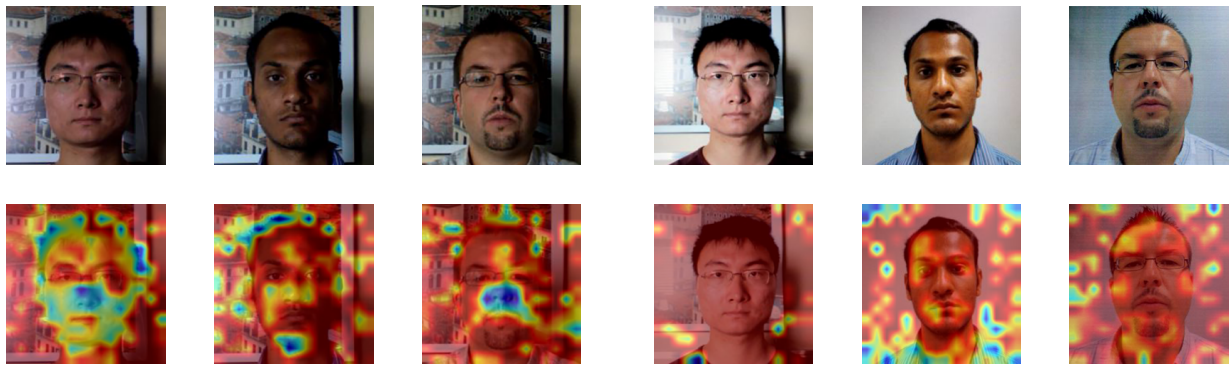


Figure 11. **Grad-Cam visualization for O&C&M to I.** On the left is a real image, and on the right is a spoof image.

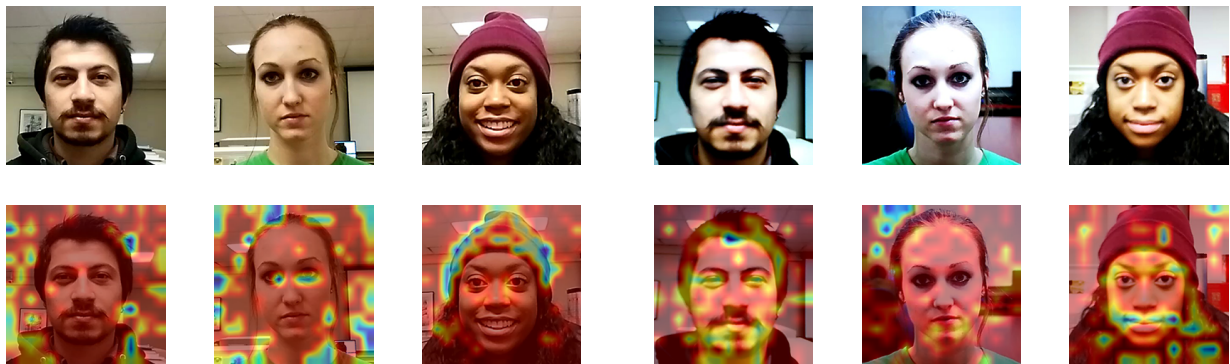


Figure 12. **Grad-Cam visualization for O&C&I to M.** On the left is a real image, and on the right is a spoof image.

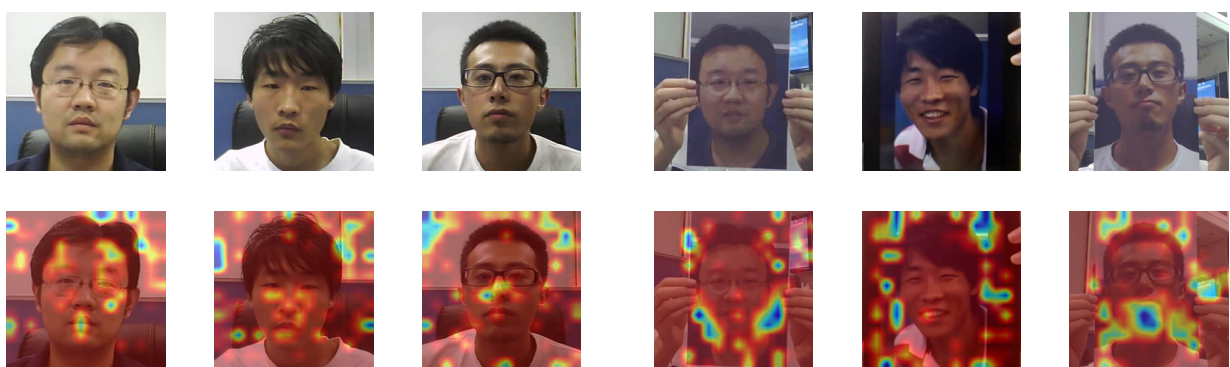


Figure 13. **Grad-Cam visualization for O&M&I to C.** On the left is a real image, and on the right is a spoof image.

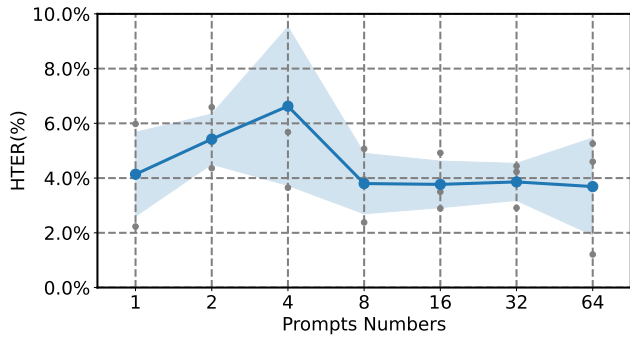


Figure 14. HTER and AUC on I&C&M to O under different text prompts number

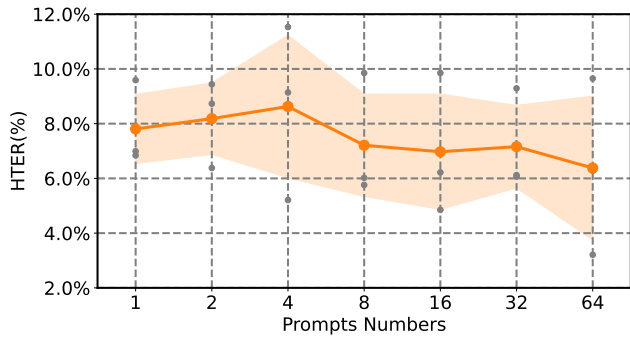


Figure 15. HTER and AUC on O&C&M to I under different text prompts number

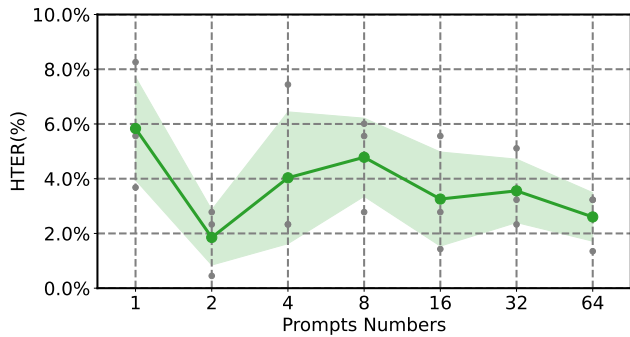


Figure 16. HTER and AUC on O&C&I to M under different text prompts number

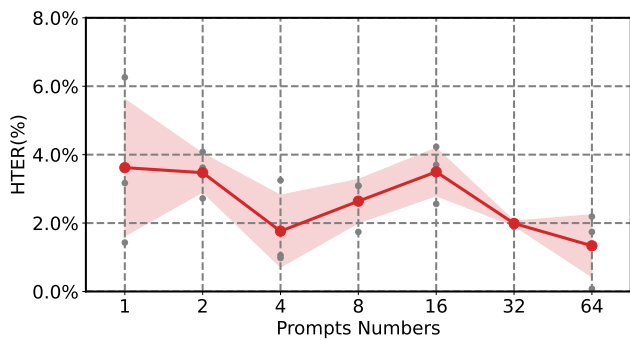


Figure 17. HTER and AUC on O&M&I to C under different text prompts number

## F. Detailed Text Prompts

### Text Prompts For Real Faces In Prompt Library

1. A real photo of a person
2. A genuine image of the person
3. An actual snapshot of the individual
4. A real-life photograph of the person
5. A true-to-life photo of the person
6. An authentic photograph of the individual
7. A bona fide picture of the person
8. An unedited photograph of the individual
9. A legitimate snapshot of the person
10. An original photo depicting the individual
11. A veritable image of the person
12. An unaltered photograph of the individual
13. A factual representation in a photo of the person
14. An honest capture of the individual's likeness
15. A straightforward photograph of the person
16. An undistorted image of the individual
17. An unembellished photograph of the individual
18. A straightforward capture of the person's appearance
19. A direct shot of the individual, unmodified
20. A candid photograph depicting the person
21. A natural, unposed photo of the individual
22. An unretouched image of the person
23. A clear, unfiltered photograph of the individual
24. A genuine representation in a photo of the person
25. An honest, unadorned picture of the individual
26. A pure, unedited image of the person
27. A real, unmanipulated photograph of the individual
28. A sincere, untouched snapshot of the person
29. An exact, unaltered capture of the individual's visage
30. An unvarnished, true photo of the person
31. An unexaggerated, straightforward image of the individual
32. A plain, accurate photograph of the person
33. A genuine, unaltered image of the person
34. A truthful depiction in a photograph of the individual
35. An unprocessed photo of the person
36. A raw, natural shot of the individual
37. A direct, unaltered photograph of the person
38. A true, unfiltered image of the individual
39. An unmanipulated representation in a photo of the person
40. A straightforward, unedited picture of the individual
41. An undisturbed, authentic photo of the person
42. An original, unenhanced image of the individual
43. A non-doctored photograph of the person
44. A pure, straightforward shot of the individual
45. An unsullied, genuine photograph of the person
46. An uncropped, clear image of the individual
47. A veracious, unaltered photo of the person
48. A true representation in a snapshot of the individual
49. An honest, unfiltered view of the person
50. A direct, unmanipulated photo of the individual
51. A natural, unaltered image of the person
52. An untouched, true-to-form photograph of the individual
53. A straightforward, unenhanced snapshot of the person
54. An unedited, authentic image of the individual
55. A clear-cut, unadulterated photo of the person
56. A non-altered, genuine representation of the individual
57. A raw, unfiltered capture of the person
58. An unadorned, straightforward picture of the individual
59. A pure, unvarnished image of the person
60. An honest, unprocessed photograph of the individual
61. A direct, undistorted snapshot of the person
62. An unedited, clear depiction of the individual
63. A truthful, unaltered photo of the person
64. An unenhanced, natural picture of the individual

---

## Text Prompts For Print Attacks In Prompt Library

1. A printed photo
2. A print attack photo
3. A printed photo with is blur and lack of details
4. A photo of an A4 paper with a face printed on it
5. An image of an A4 sheet of paper bearing a printed face
6. A photo of a paper printed with an image of a person
7. A hard copy of a photograph
8. A printed image on paper
9. A blurred and indistinct printed photo
10. A photograph depicting a face on an A4 sheet
11. An A4 paper with a facial image printed upon it
12. A paper bearing a printed photograph of an individual
13. A printout of a photo with reduced clarity and detail
14. An image of a person printed on standard paper
15. A photo print, lacking sharpness and detail, on paper
16. A snapshot printed on an A4-sized paper with a facial image
17. A low-resolution printout of a face
18. An image on paper, showing signs of being printed
19. A photocopy of a photographic image
20. A print of a digital photo, with visible pixelation
21. A face image printed on a regular sheet of paper
22. A printed photograph with faded colors
23. A photo printout showing distortion
24. A printed picture on a letter-sized paper
25. An office printer output of a face photo
26. A printed facial image with visible print lines
27. A smudged photo printout on white paper
28. A paper print of a digital image, showing compression artifacts
29. A color print of a photograph, slightly blurred
30. A printed image of a person with low contrast
31. A printout of a portrait photo on plain paper
32. A digitally printed photo with overexposure
33. A facial photo printed using a home printer
34. A printout of a photo, showing signs of ink spreading
35. A printed image, lacking in fine details
36. A photo on paper, with visible printing dots
37. A printed portrait with a grainy texture
38. A photo reproduction on matte paper
39. A photocopy of a face, with some areas washed out
40. A laser-printed image of an individual
41. An inkjet printed photo with color misalignment
42. A printed image, showing banding issues
43. A paper print showing a digitally zoomed-in face
44. A printed photo with noticeable color shifts
45. A facial photograph printed on glossy paper
46. A printout of a photo with a moiré pattern
47. A printed face photo with a skewed perspective
48. A color photo printed on a grayscale setting
49. A photocopy of a person's photo, with reduced saturation
50. A printed image of a face, slightly off-center on the paper
51. A photo print showing ink smears
52. A printed image with a noticeable paper texture
53. A photograph print with uneven ink distribution
54. A printed photo, showing reduced dynamic range
55. A face printout on textured paper
56. A photo print with a yellowish tint
57. A printed image of a person, cropped awkwardly
58. A facial photo printed with low ink levels
59. A digitally printed face with artifacts
60. A printout of a photo with a watermark
61. A printed photograph, slightly torn at the edge
62. A print of a digital photo, with color bleeding
63. A photo printed on thin, low-quality paper
64. A printout of a face, showing digital noise

---

---

## Text Prompts For Replay Attacks In Prompt Library

1. A replay attack photo
2. A photo of an iPad
3. A photo of an iPad that displaying face images
4. A photo of a display
5. A photo of a screen
6. An image of a screen
7. A photograph used for a replay attack
8. An image of an iPad
9. A photo showing an iPad displaying facial images
10. A snapshot of a digital display screen
11. A photograph capturing a computer or television screen
12. An image depicting a monitor display
13. A picture of a tablet screen showing a face
14. A photograph of a device's screen in operation
15. An image depicting a monitor display
16. A picture of a tablet screen showing a face
17. A photo of a smartphone screen displaying an image
18. An image of a laptop screen showing a face
19. A snapshot showing a monitor with a facial image
20. A photo of a device screen during a replay attack
21. An image of a screen showing a video playback
22. A photograph of a face displayed on a digital device
23. A picture capturing a face on a tablet display
24. A photo of a monitor screen with a facial portrait
25. An image of a screen replaying a video
26. A photograph showing a digital screen in use
27. A snapshot of a face being displayed on a smartphone
28. A photo of a computer monitor displaying images
29. An image of a television screen in operation
30. A picture of a digital display showing a live feed
31. A photo of an electronic display with a static image
32. An image capturing a tablet screen in operation
33. A photograph of a screen showing a streaming video
34. A snapshot of a digital billboard display
35. A photo capturing a screen with multimedia content
36. An image of a projected screen displaying a face
37. A picture of a face on a high-resolution monitor
38. A photo of a screen with high brightness showing a face
39. An image of a LED display screen in action
40. A photograph of a smartphone screen with a zoomed-in face
41. A picture showing a monitor with a live webcam feed
42. A snapshot of a TV screen showing a recorded video
43. A photo of a video call in progress on a tablet
44. An image showing a digital kiosk display
45. A photograph of a computer screen with a face slideshow
46. A picture of a mobile phone screen playing a video
47. A photo showing a digital photo frame in use
48. An image of a virtual reality screen displaying a face
49. A picture showing a computer monitor with editing software
50. A snapshot of an outdoor LED screen displaying an ad
51. A photo of a tablet screen with a live streaming app
52. An image of a monitor with a split-screen view
53. A photograph of a phone screen showing a photo gallery
54. A picture of a screen displaying interactive media
55. A photo showing a touchscreen device in use
56. An image of a monitor with screen mirroring active
57. A photograph showing a tablet with a drawing app
58. A picture of a laptop screen with a video conference
59. A snapshot of a smartwatch screen with a notification
60. A photo of a car display screen showing navigation
61. An image of a screen with augmented reality content
62. A photograph of a display with facial recognition software
63. A picture of a screen displaying a 3D model of a face
64. A photo of a digital signboard showing a portrait

---

## References

- [1] Timo Ahonen, Abdenour Hadid, and Matti Pietikainen. Face description with local binary patterns: Application to face recognition. *IEEE Transactions on Pattern Analysis and Machine Intelligence*, 28(12):2037–2041, 2006. [1](#) [2](#)
- [2] Yousef Atoum, Yaojie Liu, Amin Jourabloo, and Xiaoming Liu. Face anti-spoofing using patch and depth-based cnns. In *2017 IEEE International Joint Conference on Biometrics (IJCGB)*, pages 319–328. IEEE, 2017. [2](#)
- [3] Jimmy Lei Ba, Jamie Ryan Kiros, and Geoffrey E Hinton. Layer normalization. *arXiv preprint arXiv:1607.06450*, 2016. [4](#)
- [4] Gilles Blanchard, Gyemin Lee, and Clayton Scott. Generalizing from several related classification tasks to a new unlabeled sample. *Advances in Neural Information Processing Systems*, 24, 2011. [1](#)
- [5] Zinelabidine Boulkenafet, Jukka Komulainen, and Abdenour Hadid. Face anti-spoofing based on color texture analysis. In *2015 IEEE International Conference on Image Processing (ICIP)*, pages 2636–2640. IEEE, 2015. [1](#)
- [6] Zinelabidine Boulkenafet, Jukka Komulainen, Lei Li, Xiaoyi Feng, and Abdenour Hadid. Oulu-npu: A mobile face presentation attack database with real-world variations. In *2017 12th IEEE International Conference on Automatic Face & Gesture Recognition (FG 2017)*, pages 612–618. IEEE, 2017. [1](#), [6](#), [9](#)
- [7] Zhihong Chen, Taiping Yao, Kekai Sheng, Shouhong Ding, Ying Tai, Jilin Li, Feiyue Huang, and Xinyu Jin. Generalizable representation learning for mixture domain face anti-spoofing. In *Proceedings of the AAAI Conference on Artificial Intelligence*, pages 1132–1139, 2021. [2](#), [6](#), [7](#)
- [8] Ivana Chingovska, André Anjos, and Sébastien Marcel. On the effectiveness of local binary patterns in face anti-spoofing. In *2012 BIOSIG-proceedings of the International Conference on Biometrics Special Interest Group (BIOSIG)*, pages 1–7. IEEE, 2012. [1](#), [6](#), [9](#)
- [9] Ivana Chingovska, Andre Rabello Dos Anjos, and Sébastien Marcel. Biometrics evaluation under spoofing attacks. *IEEE Transactions on Information Forensics and Security*, 9(12):2264–2276, 2014. [6](#)
- [10] Tiago de Freitas Pereira, André Anjos, José Mario De Martino, and Sébastien Marcel. Lbp - top based countermeasure against face spoofing attacks. In *Computer Vision-ACCV 2012 Workshops: ACCV 2012 International Workshops, Daejeon, Korea, November 5-6, 2012, Revised Selected Papers, Part I* 11, pages 121–132. Springer, 2013. [1](#)
- [11] Tiago de Freitas Pereira, Jukka Komulainen, André Anjos, José Mario De Martino, Abdenour Hadid, Matti Pietikäinen, and Sébastien Marcel. Face liveness detection using dynamic texture. *EURASIP Journal on Image and Video Processing*, 2014(1):2, 2014. [6](#), [7](#)
- [12] Jiankang Deng, Jia Guo, Niannan Xue, and Stefanos Zafeiriou. Arcface: Additive angular margin loss for deep face recognition. In *Proceedings of the IEEE/CVF Conference on Computer Vision and Pattern Recognition*, pages 4690–4699, 2019. [1](#)
- [13] Alexey Dosovitskiy, Lucas Beyer, Alexander Kolesnikov, Dirk Weissenborn, Xiaohua Zhai, Thomas Unterthiner, Mostafa Dehghani, Matthias Minderer, Georg Heigold, Sylvain Gelly, et al. An image is worth 16x16 words: Transformers for image recognition at scale. *arXiv preprint arXiv:2010.11929*, 2020. [4](#)
- [14] Zhekai Du, Jingjing Li, Lin Zuo, Lei Zhu, and Ke Lu. Energy-based domain generalization for face anti-spoofing. In *Proceedings of the 30th ACM International Conference on Multimedia*, pages 1749–1757, 2022. [2](#), [6](#), [7](#)
- [15] Mohammed E Fathy, Vishal M Patel, and Rama Chellappa. Face-based active authentication on mobile devices. In *2015 IEEE International Conference on Acoustics, Speech and Signal Processing (ICASSP)*, pages 1687–1691. IEEE, 2015. [1](#)
- [16] Litong Feng, Lai-Man Po, Yuming Li, Xuyuan Xu, Fang Yuan, Terence Chun-Ho Cheung, and Kwok-Wai Cheung. Integration of image quality and motion cues for face anti-spoofing: A neural network approach. *Journal of Visual Communication and Image Representation*, 38:451–460, 2016. [1](#)
- [17] Andreas Fürst, Elisabeth Rumetshofer, Johannes Lehner, Viet T Tran, Fei Tang, Hubert Ramsauer, David Kreil, Michael Kopp, Günter Klambauer, Angela Bitto, et al. Cloob: Modern hopfield networks with infoloob outperform clip. *Advances in Neural Information Processing Systems*, 35:20450–20468, 2022. [2](#)
- [18] Kaiming He, Xiangyu Zhang, Shaoqing Ren, and Jian Sun. Deep residual learning for image recognition. In *Proceedings of the IEEE Conference on Computer Vision and Pattern Recognition*, pages 770–778, 2016. [4](#)
- [19] Xun Huang and Serge Belongie. Arbitrary style transfer in real-time with adaptive instance normalization. In *Proceedings of the IEEE International Conference on Computer Vision*, pages 1501–1510, 2017. [1](#)
- [20] Yunpei Jia, Jie Zhang, Shiguang Shan, and Xilin Chen. Single-side domain generalization for face anti-spoofing. In *Proceedings of the IEEE/CVF Conference on Computer Vision and Pattern Recognition (CVPR)*, 2020. [1](#), [2](#), [6](#), [7](#), [11](#)
- [21] Yunpei Jia, Jie Zhang, Shiguang Shan, and Xilin Chen. Unified unsupervised and semi-supervised domain adaptation network for cross-scenario face anti-spoofing. *Pattern Recognition*, 115:107888, 2021. [1](#)
- [22] Alexander Kirillov, Eric Mintun, Nikhila Ravi, Hanzi Mao, Chloe Rolland, Laura Gustafson, Tete Xiao, Spencer Whitehead, Alexander C Berg, Wan-Yen Lo, et al. Segment anything. *arXiv preprint arXiv:2304.02643*, 2023. [2](#)
- [23] Jukka Komulainen, Abdenour Hadid, and Matti Pietikäinen. Context based face anti-spoofing. In *2013 IEEE Sixth International Conference on Biometrics: Theory, Applications and Systems (BTAS)*, pages 1–8. IEEE, 2013. [1](#)
- [24] Neslihan Kose and Jean-Luc Dugelay. Shape and texture based countermeasure to protect face recognition systems against mask attacks. In *Proceedings of the IEEE Conference on Computer Vision and Pattern Recognition Workshops*, pages 111–116, 2013. [1](#)
- [25] Haoliang Li, Wen Li, Hong Cao, Shiqi Wang, Feiyue Huang, and Alex C Kot. Unsupervised domain adaptation for face

anti-spoofing. *IEEE Transactions on Information Forensics and Security*, 13(7):1794–1809, 2018. 1, 2

[26] Haoliang Li, Sinno Jialin Pan, Shiqi Wang, and Alex C Kot. Domain generalization with adversarial feature learning. In *Proceedings of the IEEE Conference on Computer Vision and Pattern Recognition*, pages 5400–5409, 2018. 6, 7

[27] Junnan Li, Ramprasaath Selvaraju, Akhilesh Gotmare, Shafiq Joty, Caiming Xiong, and Steven Chu Hong Hoi. Align before fuse: Vision and language representation learning with momentum distillation. *Advances in Neural Information Processing Systems*, 34:9694–9705, 2021. 2

[28] Junnan Li, Dongxu Li, Caiming Xiong, and Steven Hoi. Blip: Bootstrapping language-image pre-training for unified vision-language understanding and generation. In *International Conference on Machine Learning*, pages 12888–12900. PMLR, 2022. 2, 4, 10

[29] Yangguang Li, Feng Liang, Lichen Zhao, Yufeng Cui, Wanli Ouyang, Jing Shao, Fengwei Yu, and Junjie Yan. Supervision exists everywhere: A data efficient contrastive language-image pre-training paradigm. *arXiv preprint arXiv:2110.05208*, 2021. 2

[30] Chen-Hao Liao, Wen-Cheng Chen, Hsuan-Tung Liu, Yi-Ren Yeh, Min-Chun Hu, and Chu-Song Chen. Domain invariant vision transformer learning for face anti-spoofing. In *Proceedings of the IEEE/CVF Winter Conference on Applications of Computer Vision*, pages 6098–6107, 2023. 2, 6, 7, 11

[31] Zhiqiu Lin, Samuel Yu, Zhiyi Kuang, Deepak Pathak, and Deva Ramanan. Multimodality helps unimodality: Cross-modal few-shot learning with multimodal models. In *Proceedings of the IEEE/CVF Conference on Computer Vision and Pattern Recognition (CVPR)*, pages 19325–19337, 2023. 4

[32] Zhiqiu Lin, Samuel Yu, Zhiyi Kuang, Deepak Pathak, and Deva Ramanan. Multimodality helps unimodality: Cross-modal few-shot learning with multimodal models. In *Proceedings of the IEEE/CVF Conference on Computer Vision and Pattern Recognition*, pages 19325–19337, 2023. 3

[33] Ajian Liu, Chenxu Zhao, Zitong Yu, Jun Wan, Anyang Su, Xing Liu, Zichang Tan, Sergio Escalera, Junliang Xing, Yanyan Liang, et al. Contrastive context-aware learning for 3d high-fidelity mask face presentation attack detection. *IEEE Transactions on Information Forensics and Security*, 17:2497–2507, 2022. 1

[34] Huidong Liu, Shaoyuan Xu, Jinmiao Fu, Yang Liu, Ning Xie, Chien-Chih Wang, Bryan Wang, and Yi Sun. Cma-clip: Cross-modality attention clip for image-text classification. *arXiv preprint arXiv:2112.03562*, 2021. 3

[35] Shubao Liu, Ke-Yue Zhang, Taiping Yao, Mingwei Bi, Shouhong Ding, Jilin Li, Feiyue Huang, and Lizhuang Ma. Adaptive normalized representation learning for generalizable face anti-spoofing. In *Proceedings of the 29th ACM International Conference on Multimedia*, pages 1469–1477, 2021. 1, 2, 6, 7

[36] Shubao Liu, Ke-Yue Zhang, Taiping Yao, Kekai Sheng, Shouhong Ding, Ying Tai, Jilin Li, Yuan Xie, and Lizhuang Ma. Dual reweighting domain generalization for face presentation attack detection. *arXiv preprint arXiv:2106.16128*, 2021. 1, 2, 6, 7

[37] Ze Liu, Yutong Lin, Yue Cao, Han Hu, Yixuan Wei, Zheng Zhang, Stephen Lin, and Baining Guo. Swin transformer: Hierarchical vision transformer using shifted windows. In *Proceedings of the IEEE/CVF International Conference on Computer Vision*, pages 10012–10022, 2021. 4

[38] Ze Liu, Han Hu, Yutong Lin, Zhuliang Yao, Zhenda Xie, Yixuan Wei, Jia Ning, Yue Cao, Zheng Zhang, Li Dong, et al. Swin transformer v2: Scaling up capacity and resolution. In *Proceedings of the IEEE/CVF Conference on Computer Vision and Pattern Recognition*, pages 12009–12019, 2022. 4

[39] Mingsheng Long, Yue Cao, Jianmin Wang, and Michael Jordan. Learning transferable features with deep adaptation networks. In *International Conference on Machine Learning*, pages 97–105. PMLR, 2015. 1

[40] Mingsheng Long, Han Zhu, Jianmin Wang, and Michael I Jordan. Deep transfer learning with joint adaptation networks. In *International Conference on Machine Learning*, pages 2208–2217. PMLR, 2017. 1

[41] Jukka Määttä, Abdenour Hadid, and Matti Pietikäinen. Face spoofing detection from single images using micro-texture analysis. In *2011 International Joint Conference on Biometrics (IJCB)*, pages 1–7. IEEE, 2011. 1, 2

[42] Jukka Määttä, Abdenour Hadid, and Matti Pietikäinen. Face spoofing detection from single images using micro-texture analysis. In *2011 International Joint Conference on Biometrics (IJCB)*, pages 1–7. IEEE, 2011. 6, 7

[43] Ishan Manjani, Snigdha Tariyal, Mayank Vatsa, Richa Singh, and Angshul Majumdar. Detecting silicone mask-based presentation attack via deep dictionary learning. *IEEE Transactions on Information Forensics and Security*, 12(7):1713–1723, 2017. 1

[44] Sachit Menon and Carl Vondrick. Visual classification via description from large language models. *arXiv preprint arXiv:2210.07183*, 2022. 3

[45] Xuesong Niu, Zitong Yu, Hu Han, Xiaobai Li, Shiguang Shan, and Guoying Zhao. Video-based remote physiological measurement via cross-verified feature disentangling. In *Computer Vision–ECCV 2020: 16th European Conference, Glasgow, UK, August 23–28, 2020, Proceedings, Part II 16*, pages 295–310. Springer, 2020. 1, 2

[46] OpenAI. Gpt-4 technical report, 2023. 3, 9

[47] Gang Pan, Lin Sun, Zhaohui Wu, and Shihong Lao. Eyeblink-based anti-spoofing in face recognition from a generic webcamera. In *2007 IEEE 11th International Conference on Computer Vision*, pages 1–8. IEEE, 2007. 1

[48] Keyurkumar Patel, Hu Han, Anil K Jain, and Greg Ott. Live face video vs. spoof face video: Use of moiré patterns to detect replay video attacks. In *2015 International Conference on Biometrics (ICB)*, pages 98–105. IEEE, 2015. 4

[49] Keyurkumar Patel, Hu Han, and Anil K Jain. Secure face unlock: Spoof detection on smartphones. *IEEE Transactions on Information Forensics and Security*, 11(10):2268–2283, 2016. 1, 2

[50] Bruno Peixoto, Carolina Michelassi, and Anderson Rocha. Face liveness detection under bad illumination conditions. In *2011 18th IEEE International Conference on Image Processing*, pages 3557–3560. IEEE, 2011. 1

[51] Daniel Pérez-Cabo, David Jiménez-Cabello, Artur Costa-Pazo, and Roberto J López-Sastre. Learning to learn face-pad: a lifelong learning approach. In *2020 IEEE International Joint Conference on Biometrics (IJCB)*, pages 1–9. IEEE, 2020. [6](#)

[52] Allan Pinto, William Robson Schwartz, Helio Pedrini, and Anderson de Rezende Rocha. Using visual rhythms for detecting video-based facial spoof attacks. *IEEE Transactions on Information Forensics and Security*, 10(5):1025–1038, 2015. [1](#)

[53] Sarah Pratt, Ian Covert, Rosanne Liu, and Ali Farhadi. What does a platypus look like? generating customized prompts for zero-shot image classification. In *Proceedings of the IEEE/CVF International Conference on Computer Vision*, pages 15691–15701, 2023. [3](#)

[54] Yunxiao Qin, Chenxu Zhao, Xiangyu Zhu, Zezheng Wang, Zitong Yu, Tianyu Fu, Feng Zhou, Jingping Shi, and Zhen Lei. Learning meta model for zero-and few-shot face anti-spoofing. In *Proceedings of the AAAI Conference on Artificial Intelligence*, pages 11916–11923, 2020. [6](#)

[55] Ruijie Quan, Yu Wu, Xin Yu, and Yi Yang. Progressive transfer learning for face anti-spoofing. *IEEE Transactions on Image Processing*, 30:3946–3955, 2021. [1](#)

[56] Alec Radford, Jong Wook Kim, Chris Hallacy, Aditya Ramesh, Gabriel Goh, Sandhini Agarwal, Girish Sastry, Amanda Askell, Pamela Mishkin, Jack Clark, et al. Learning transferable visual models from natural language supervision. In *International Conference on Machine Learning*, pages 8748–8763. PMLR, 2021. [2, 4, 5, 7, 9, 10](#)

[57] Rasha Khudiar Rija, Ghaida Muttasher, and Ahmed Al-Araji. Payment systems based on face recognition: A survey. *Journal of Optoelectronics Laser*, 41(5):563–571, 2022. [1](#)

[58] Florian Schroff, Dmitry Kalenichenko, and James Philbin. Facenet: A unified embedding for face recognition and clustering. In *Proceedings of the IEEE Conference on Computer Vision and Pattern Recognition*, pages 815–823, 2015. [1](#)

[59] Ramprasaath R Selvaraju, Michael Cogswell, Abhishek Das, Ramakrishna Vedantam, Devi Parikh, and Dhruv Batra. Grad-cam: Visual explanations from deep networks via gradient-based localization. In *Proceedings of the IEEE International Conference on Computer Vision*, pages 618–626, 2017. [7, 8, 11](#)

[60] Rui Shao, Xiangyuan Lan, Jiawei Li, and Pong C Yuen. Multi-adversarial discriminative deep domain generalization for face presentation attack detection. In *Proceedings of the IEEE/CVF Conference on Computer Vision and Pattern recognition*, pages 10023–10031, 2019. [1, 2, 6, 7, 11](#)

[61] Rui Shao, Xiangyuan Lan, and Pong C Yuen. Regularized fine-grained meta face anti-spoofing. In *Proceedings of the AAAI Conference on Artificial Intelligence*, pages 11974–11981, 2020. [2, 6, 7](#)

[62] Ludwig Slusky. Cybersecurity of online proctoring systems. *Journal of International Technology and Information Management*, 29(1):56–83, 2020. [1](#)

[63] Koushik Srivatsan, Muzammal Naseer, and Karthik Nandakumar. Flip: Cross-domain face anti-spoofing with language guidance. In *Proceedings of the IEEE/CVF International Conference on Computer Vision (ICCV)*, pages 19685–19696, 2023. [2, 7](#)

[64] Yiyou Sun, Yaojie Liu, Xiaoming Liu, Yixuan Li, and Wen-Sheng Chu. Rethinking domain generalization for face anti-spoofing: Separability and alignment. In *Proceedings of the IEEE/CVF Conference on Computer Vision and Pattern Recognition*, pages 24563–24574, 2023. [7](#)

[65] Yaniv Taigman, Ming Yang, Marc’Aurelio Ranzato, and Lior Wolf. Deepface: Closing the gap to human-level performance in face verification. In *Proceedings of the IEEE conference on computer vision and pattern recognition*, pages 1701–1708, 2014. [1](#)

[66] Xiaoyang Tan, Yi Li, Jun Liu, and Lin Jiang. Face liveness detection from a single image with sparse low rank bilinear discriminative model. In *Computer Vision–ECCV 2010: 11th European Conference on Computer Vision, Heraklion, Crete, Greece, September 5–11, 2010, Proceedings, Part VI 11*, pages 504–517. Springer, 2010. [1](#)

[67] Laurens Van der Maaten and Geoffrey Hinton. Visualizing data using t-sne. *Journal of machine learning research*, 9(11), 2008. [8, 11](#)

[68] Ashish Vaswani, Noam Shazeer, Niki Parmar, Jakob Uszkoreit, Llion Jones, Aidan N Gomez, Łukasz Kaiser, and Illia Polosukhin. Attention is all you need. *Advances in neural information processing systems*, 30, 2017. [4](#)

[69] Guoqing Wang, Hu Han, Shiguang Shan, and Xilin Chen. Improving cross-database face presentation attack detection via adversarial domain adaptation. In *2019 International Conference on Biometrics (ICB)*, pages 1–8. IEEE, 2019. [1](#)

[70] Jingjing Wang, Jingyi Zhang, Ying Bian, Youyi Cai, Chunmao Wang, and Shiliang Pu. Self-domain adaptation for face anti-spoofing. In *Proceedings of the AAAI Conference on Artificial Intelligence*, pages 2746–2754, 2021. [1, 2](#)

[71] Mei Wang and Weihong Deng. Deep visual domain adaptation: A survey. *Neurocomputing*, 312:135–153, 2018. [1](#)

[72] Zhuo Wang, Qiangchang Wang, Weihong Deng, and Guodong Guo. Learning multi-granularity temporal characteristics for face anti-spoofing. *IEEE Transactions on Information Forensics and Security*, 17:1254–1269, 2022. [1](#)

[73] Zhuo Wang, Zezheng Wang, Zitong Yu, Weihong Deng, Jiahong Li, Tingting Gao, and Zhongyuan Wang. Domain generalization via shuffled style assembly for face anti-spoofing. In *Proceedings of the IEEE/CVF Conference on Computer Vision and Pattern Recognition*, pages 4123–4133, 2022. [1, 2, 6, 7, 11](#)

[74] Di Wen, Hu Han, and Anil K Jain. Face spoof detection with image distortion analysis. *IEEE Transactions on Information Forensics and Security*, 10(4):746–761, 2015. [1, 6, 9](#)

[75] Jianwei Yang, Zhen Lei, Shengcui Liao, and Stan Z Li. Face liveness detection with component dependent descriptor. In *2013 International Conference on Biometrics (ICB)*, pages 1–6. IEEE, 2013. [1](#)

[76] Jianwei Yang, Zhen Lei, and Stan Z Li. Learn convolutional neural network for face anti-spoofing. *arXiv preprint arXiv:1408.5601*, 2014. [1](#)

[77] Zitong Yu, Xiaobai Li, Xuesong Niu, Jingang Shi, and Guoying Zhao. Face anti-spoofing with human material perception.

In *Computer Vision–ECCV 2020: 16th European Conference, Glasgow, UK, August 23–28, 2020, Proceedings, Part VII 16*, pages 557–575. Springer, 2020. 2

[78] Zitong Yu, Jun Wan, Yunxiao Qin, Xiaobai Li, Stan Z Li, and Guoying Zhao. Nas-fas: Static-dynamic central difference network search for face anti-spoofing. *IEEE Transactions on Pattern Analysis and Machine Intelligence*, 43(9):3005–3023, 2020. 1

[79] Zitong Yu, Chenxu Zhao, Zezheng Wang, Yunxiao Qin, Zhuo Su, Xiaobai Li, Feng Zhou, and Guoying Zhao. Searching central difference convolutional networks for face anti-spoofing. In *Proceedings of the IEEE/CVF Conference on Computer Vision and Pattern Recognition*, pages 5295–5305, 2020. 1

[80] Zitong Yu, Xiaobai Li, Jingang Shi, Zhaoqiang Xia, and Guoying Zhao. Revisiting pixel-wise supervision for face anti-spoofing. *IEEE Transactions on Biometrics, Behavior, and Identity Science*, 3(3):285–295, 2021.

[81] Zitong Yu, Yunxiao Qin, Hengshuang Zhao, Xiaobai Li, and Guoying Zhao. Dual-cross central difference network for face anti-spoofing. *arXiv preprint arXiv:2105.01290*, 2021. 1

[82] Zitong Yu, Yunxiao Qin, Xiaobai Li, Chenxu Zhao, Zhen Lei, and Guoying Zhao. Deep learning for face anti-spoofing: A survey. *IEEE Transactions on Pattern Analysis and Machine Intelligence*, 45(5):5609–5631, 2022. 1

[83] Yuanhan Zhang, Zhenfei Yin, Yidong Li, Guojun Yin, Junjie Yan, Jing Shao, and Ziwei Liu. Celeba-spoof: Large-scale face anti-spoofing dataset with rich annotations. In *European Conference on Computer Vision (ECCV)*, 2020. 7

[84] Yuanhan Zhang, ZhenFei Yin, Yidong Li, Guojun Yin, Junjie Yan, Jing Shao, and Ziwei Liu. Celeba-spoof: Large-scale face anti-spoofing dataset with rich annotations. In *Computer Vision–ECCV 2020: 16th European Conference, Glasgow, UK, August 23–28, 2020, Proceedings, Part XII 16*, pages 70–85. Springer, 2020. 1

[85] Zhiwei Zhang, Junjie Yan, Sifei Liu, Zhen Lei, Dong Yi, and Stan Z Li. A face antispoofing database with diverse attacks. In *2012 5th IAPR International Conference on Biometrics (ICB)*, pages 26–31. IEEE, 2012. 1, 6, 9

[86] Junwei Zhou, Ke Shu, Dongdong Zhao, and Zhe Xia. Domain adaptation based person-specific face anti-spoofing using color texture features. In *Proceedings of the 2020 5th International Conference on Machine Learning Technologies*, pages 79–85, 2020. 1, 2

[87] Kaiyang Zhou, Ziwei Liu, Yu Qiao, Tao Xiang, and Chen Change Loy. Domain generalization: A survey. *IEEE Transactions on Pattern Analysis and Machine Intelligence*, 2022. 1

[88] Qianyu Zhou, Ke-Yue Zhang, Taiping Yao, Ran Yi, Shouhong Ding, and Lizhuang Ma. Adaptive mixture of experts learning for generalizable face anti-spoofing. In *Proceedings of the 30th ACM International Conference on Multimedia*, pages 6009–6018, 2022. 1, 2, 6, 7

[89] Qianyu Zhou, Ke-Yue Zhang, Taiping Yao, Ran Yi, Kekai Sheng, Shouhong Ding, and Lizhuang Ma. Generative domain adaptation for face anti-spoofing. In *European Conference on Computer Vision*, pages 335–356. Springer, 2022. 1, 2

[90] Qianyu Zhou, Ke-Yue Zhang, Taiping Yao, Xuequan Lu, Ran Yi, Shouhong Ding, and Lizhuang Ma. Instance-aware domain generalization for face anti-spoofing. *arXiv preprint arXiv:2304.05640*, 2023. 1, 2, 6, 7, 11